

**Title: Simultaneous disintegration of outlet glaciers in Porpoise Bay (Wilkes Land),
East Antarctica, driven by sea-ice break-up.**

Authors: B.W.J. Miles^{1*}, C. R. Stokes¹, S.S.R. Jamieson¹

Affiliation: ¹*Department of Geography, Durham University, Science Site, South Road, Durham, DH1 3LE,
UK*

**Correspondence to: a.w.j.miles@durham.ac.uk*

Abstract: The floating ice shelves and glacier tongues which fringe the Antarctic continent are important because they help buttress ice flow from the ice sheet interior. Dynamic feedbacks associated with glacier calving have the potential to reduce buttressing and subsequently increase ice flow into the ocean. However, there are few high temporal resolution studies on glacier calving, especially in East Antarctica. Here we use ENVISAT ASAR wide swath mode imagery to investigate monthly glacier terminus change across six marine-terminating outlet glaciers in Porpoise Bay (-76°S, 128°E), Wilkes Land (East Antarctica), between November 2002 and March 2012. This reveals a large near-simultaneous calving event in January 2007, resulting in a total of ~2,900 km² of ice being removed from glacier tongues. We also observe the start of a similar large near-simultaneous calving event in March 2016. Our observations suggest that both of these large calving events are driven by the break-up of the multi-year sea-ice which usually occupies Porpoise Bay. However, these break-up events appear to have been driven by contrasting mechanisms. We link the 2007 sea-ice break-up to atmospheric circulation anomalies in December 2005 weakening the multi-year sea-ice through a combination of surface melt and a change in wind direction prior to its eventual break-up in January 2007. In contrast, the 2016 break-up event is linked to the terminus of Holmes (West) Glacier pushing the multi-year sea-ice further into the open ocean, making the sea-ice more vulnerable to break-up. In the context of predicted future warming and the sensitivity of sea-ice to changes in climate, our results highlight the importance of interactions between landfast sea-ice and glacier tongue stability in East Antarctica.

1. Introduction

Iceberg calving is an important process that accounts for around 50% of total mass loss to the ocean in Antarctica (Depoorter et al., 2013; Rignot et al., 2013). Moreover, dynamic feedbacks associated with retreat and/or thinning of buttressing ice shelves or floating glacier tongues can result in an increased discharge of ice into the ocean (Rott et al., 2002; Rignot et al., 2004; Wuite et al., 2015). At present, calving dynamics are only partially understood (Benn et al., 2007; Chapuis and Tetzlaff, 2014) and models struggle to replicate observed calving rates (van der Veen, 2002; Astrom et al., 2014). Therefore, improving our understanding of the mechanisms driving glacier calving and how glacier calving cycles have responded to recent changes in the ocean-climate system is important in the context of future ice sheet mass balance and sea level.

Calving is a two-stage process that requires both the initial ice fracture and the subsequent transport of the detached iceberg away from the calving front (Bassis and Jacobs, 2013). In Antarctica, major calving events can be broadly classified into two categories: the discrete detachment of large tabular icebergs (e.g. Mertz glacier tongue: Massom et al., 2015) or the spatially extensive disintegration of floating glacier tongues or ice shelves into numerous smaller icebergs (e.g. Larsen A & B ice shelves (Rott et al., 1996; Scambos et al., 2009). Observations of decadal-scale changes in glacier terminus position in both the Antarctic Peninsula and East Antarctica have suggested that despite some degree of stochasticity, iceberg calving and glacier advance/retreat is likely driven by external climatic forcing (Cook et al., 2005; Miles et al., 2013). However, despite some well-documented ice shelf collapses (Scambos et al., 2003; Banwell et al., 2013) and major individual calving events (Masson et al., 2015) there is a paucity of data on the nature and timing of calving from glaciers in Antarctica (e.g. compared to Greenland: Moon and Joughin, 2008; Carr et al., 2013), and particularly in East Antarctica.

Following recent work that highlighted the potential vulnerability of the East Antarctic Ice Sheet in Wilkes Land to ocean-climate forcing and marine ice sheet instability (Greenbaum et al., 2015; Aitken et al., 2016; Miles et al., 2013; 2016), we analyse the recent calving activity of six outlet glaciers in the Porpoise Bay region using monthly satellite imagery between November 2002 and March 2012. In addition, we also observe the start of a large calving event in 2016. We then turn our attention to investigating the drivers behind the observed calving dynamics.

2. Study area

Porpoise Bay (-76°S , 128°E) is situated in Wilkes Land, East Antarctica, approximately 300 km east of Moscow University Ice Shelf and 550 km east of Totten glacier (Fig. 1). This area was selected because it occupies a central position in Wilkes Land, which is thought to have experienced mass loss over the past decade (King et al., 2012; Sasgen et al., 2013; McMillan et al., 2014), and which is the only region of East Antarctica where the majority of marine-terminating outlet glaciers have experienced recent (2000-2012) retreat (Miles et al., 2016). This is particularly concerning because Wilkes Land overlies the Aurora subglacial basin and, due its reverse bed slope and deep troughs (Young et al., 2011), it may have been susceptible to unstable grounding line retreat in the past (Cook et al., 2014), and could make significant contributions to global sea level in the future (DeConto and Pollard, 2016). However, despite some analysis on glacier terminus position on a decadal timescales (Frezzotti and Polizzi, 2002; Miles et al., 2013; 2016), there has yet to be any investigation of inter-annual and sub-annual changes in terminus position and calving activity in the region.

Porpoise Bay is 150 km wide and is typically filled with land-fast multi-year sea-ice (Fraser et al., 2012). In total, six glaciers were analysed, with glacier velocities (from Rignot et al., 2011) ranging from $\sim 440 \text{ m yr}^{-1}$ (Sandford Glacier) to $\sim 2000 \text{ m yr}^{-1}$ (Frost Glacier). Recent studies have suggested that the largest (by width) glacier feeding into the bay - Holmes Glacier - has been thinning over the past decade (Pritchard et al., 2009; McMillan et al., 2014).

3. Methods

3.1 Satellite imagery and terminus position change

Glacier terminus positions were mapped at approximately monthly intervals between November 2002 and March 2012, using Envisat Advanced Synthetic Aperture Radar (ASAR) Wide Swath Mode (WSM) imagery across six glaciers, which were identified from the Rignot et al. (2011b) ice velocity dataset (Fig.1). Additional sub-monthly imagery between December 2006 and April 2007 were used to gain a higher temporal resolution following the identification of a major calving event around that time. During the preparation for this manuscript we also observe the start of another large calving event, which we use Sentinel-1 imagery to monitor its progress (Table 1).

Approximately 65% of all glacier frontal measurements were made using an automated mapping method. This was achieved by automatically classifying glacier tongues and sea-ice into polygons based on their pixel values, with the boundary between the two taken as the terminus position. The threshold between glacial ice and sea-ice was calculated automatically based on the image pixel statistics. In images where the automated method was unsuccessful, terminus position was mapped manually. The majority of these manual measurements were undertaken in the austral summer (December – February) when automated classification was especially problematic due to the high variability in backscatter on glacier tongues as a result of surface melt. Following the mapping of the glacier termini, length changes were calculated using the box method (Moon and Joughin, 2008). This method calculates the glacier area change between each time step divided by the width of the glacier, to give an estimation of glacier length change. The width of glacier was obtained by a reference box which approximately delineates the sides of the glacier.

Given the nature of the heavily fractured glacier fronts and the moderate resolution of Envisat ASAR WSM imagery (80 m) it was sometimes difficult to establish if individual or blocks of icebergs were attached to the glacier tongue. As a result, there are errors in precisely determining terminus change on a monthly time-scale ($\sim \pm 500$ m). However, because our focus is on major calving events, absolute terminus position is less important than the identification of major episodes of calving activity. Indeed, because estimations of terminus position were made at approximately monthly intervals, calving events were easily distinguished because the following month's estimation of terminus position would clearly show the glacier terminus in a retreated position. In addition, each image was also checked visually to make sure no small calving events were missed (i.e. as indicated by the presence of icebergs proximal to the glacier tongue).

3.2 Sea-ice

Sea-ice concentrations in Porpoise Bay were calculated using mean monthly Bootstrap sea-ice concentrations derived from the Nimbus-7 satellite and the Defence Meteorological Satellite Program (DMSP) satellites which offers near complete coverage between October 1978 and December 2014 (Comiso, 2014; <http://nsidc.org/data/nsidc-0079>). To extend the sea-ice record, we also use mean monthly Nimbus-5 Electrically Scanning Microwave Radiometer (ESMR) derived sea-ice concentrations (Parkinson et al., 2004; https://nsidc.org/data/docs/daac/nsidc0009_esmr_seaice.gd.html), which offer coverage

between December 1972 and March 1977. However, from March to May 1973, August 1973, April 1974 and June to August 1975, mean monthly sea-ice concentrations were not available. Sea-ice concentrations were extracted from 18 grid cells, covering 11,250 km² that extended across Porpoise Bay, but not into the extended area beyond the limits of the bay (Fig. 1). Grid cells which were considered likely to be filled with glacial ice were excluded. Pack ice concentrations were also extracted from a 250 x 150 km polygon adjacent to Porpoise Bay. The dataset has a spatial resolution of 25 km and monthly sea-ice concentration anomalies were calculated from the 1972-2016 monthly mean.

Daily sea-ice concentrations derived from the Artist Sea-Ice (ASI) algorithm from Advanced Microwave Scanning Radiometer - EOS (AMSR-E) data (Spreen et al., 2008) were used to calculate daily sea-ice concentration anomalies during the January 2007 sea-ice break-up (<http://icdc.zmaw.de/1/daten/cryosphere/seaiceconcentration-asi-amsre.html>). This dataset was used because it provides a higher spatial resolution (6.25 km) compared to those available using Bootstrap derived concentrations (25 km). This is important because it provides a more accurate representation of when sea-ice break-up was initiated and, due to its much higher spatial resolution, it provides data from much closer to the glacier termini (see Fig.1).

3.3 RACMO

We used the Regional Atmospheric Climate Model (RACMO) V2.3 (van Wessem et al., 2014) to simulate daily surface melt fluxes in the study area between 1979 and 2015 at a 27 km spatial resolution. The melt values were extracted from floating glacier tongues in Porpoise Bay because the model masks out sea-ice, equating to seven grid points. The absolute surface melt values are likely to be different on glacial ice, compared to the sea-ice, but the relative magnitude of melt is likely to be similar temporally.

3.4 ERA-interim

In the absence of weather stations in the vicinity of Porpoise Bay we use the 0.25° ERA-interim reanalysis dataset (<http://apps.ecmwf.int/datasets/data/interim-full-moda/levtype=sfc/>) to calculate mean monthly wind field and sea surface temperature (SST) anomalies, with respect to the 1979-2015 monthly mean. Wind field anomalies were calculated by using the mean monthly 10 m zonal (U) and meridional (V) wind components. We also used the daily 10 m zonal (U) and meridional (V) components to simulate wind field

vectors in Porpoise Bay on January 11th 2007 and March 19th 2016 which are the estimated dates of sea-ice break-up.

4. Results

4.1 Terminus position change

Analysis of glacier terminus position change of six glaciers in Porpoise Bay between November 2002 and March 2012 reveals three broad patterns of glacier change (Fig. 2). The first pattern is shown by Holmes (West) glacier, which advances a total of ~13 km throughout the observation period, with no evidence of any major iceberg calving that resulted in substantial retreat of the terminus beyond the measurement error (± 500 m). The second is shown by Sandford Glacier tongue, which advanced ~1.5 km into the ocean between November 2002 and April 2006, before its floating tongue broke away in May 2006. A further smaller calving event was observed in January 2009. Overall, by the end of the study period, its terminus had retreated around 1 km from its position in November 2002. The third pattern is shown by Frost Glacier, Glacier 1, Glacier 2 and Holmes (East) glaciers, which all advanced between November 2002 and January 2007, albeit with a small calving event in Frost glacier in May 2006. However, between January and April 2007, Frost Glacier, Glacier 1, Glacier 2 and Holmes (East) glaciers all underwent a large near-simultaneous calving event. This led to 1,300 km² of ice being removed from glaciers in Porpoise Bay, although we also note the disintegration of a major tongue from an unnamed glacier further west, which contributed a further 1,600 km². Thus, in a little over three months, a total of 2,900 km² of ice was removed from glacier tongues in the study area (Fig. 3). Following this calving event, the fronts of these glaciers stabilised and began advancing at a steady rate until the end of the study period (March, 2012) (Fig. 2), with the exception of Frost glacier which underwent a small calving event in April 2010.

4.2 Evolution of the 2007 calving event

A series of eight sub-monthly images between December 11th 2006 and April 8th 2007 show the evolution of the 2007 calving event (Fig. 4). Between December 11th 2006 and January 2nd 2007, the land-fast sea-ice edge retreats past Sandford glacier to the edge of Frost glacier and there is some evidence of sea-ice fracturing in front of the terminus of Glacier 2 (Fig. 4b). From January 2nd to January 9th a small section (~40 km²) of calved ice broke away from Frost glacier, approximately in line with the retreat edge of land-fast sea-ice (Fig. 4c). By January

25th, significant fracturing in the land-fast sea-ice had developed, and detached icebergs from Frost, Glacier 1, Glacier 2 and Holmes East glaciers begin to breakaway (Fig. 4d). This process of rapid sea-ice breakup in the east section of the bay and the disintegration of sections of Frost glacier, Glacier 1, Glacier 2 and Holmes East glaciers continues up to March 10th 2007 (Fig. 4g). In contrast, the west section of Porpoise Bay remains covered in sea-ice in front of Holmes west glacier, which does not calve throughout this event. By April 8th, the calving event had ended with a large number of calved icebergs now occupying the bay (Fig. 4h).

4.3 2016 calving event

During the preparation of this manuscript satellite observations of Porpoise Bay revealed another large near-simultaneous disintegration of glacier tongues in Porpoise Bay is currently underway. This event was initiated on March 19th where the edge of the multi-year sea-ice retreated to the Holmes West glacier terminus, removing multi-year sea-ice which was at least 14 years old. By March 24th this had led to the rapid disintegration of an 800 km² section of the Holmes West glacier tongue (Fig. 5). This was the first observed calving of Holmes (West) glacier at any stage between November 2002 and March 2016. Throughout March and April the break-up of sea-ice continued and by May 13th it had propagated to the terminus of Frost Glacier, resulting in the disintegration of large section of its tongue (Fig. 6). By 24th July sea-ice had been removed from all glacier termini in Porpoise Bay at some point during the event, resulting in a total of ~2,200 km² ice being removed from glacier tongues (Fig. 6).

4.4. The link between sea-ice and calving in Porpoise Bay

Analysis of mean monthly sea-ice concentration anomalies in Porpoise Bay between November 2002 and June 2016 (Fig. 7) reveals a major negative sea-ice anomaly occurred between January and June 2007, where monthly sea-ice concentrations were between 35% and 40% below average. This is the only noticeable (>20%) negative ice anomaly in Porpoise Bay and it coincides with the major January 2007 calving event (see Fig. 4). However, despite satellite imagery showing the break-up of sea-ice prior to the 2016 calving event (Fig. 5 and 6), in a similar manner to that in 2007 (e.g. Fig. 4), no large negative anomaly is present in the sea-ice concentration data. This is likely to reflect the production of a large armada of icebergs following the disintegration of Holmes (West) Glacier (e.g. Fig. 6), helping promote a rapid sea-ice reformation in the vicinity of Porpoise Bay. Furthermore, we note that the smaller calving events of Sandford and Frost glaciers all take place after sea-ice

had retreated away from the glacier terminus (Fig. 8). Indeed, throughout the study period, there is no evidence of any calving events taking place with sea-ice proximal to glacier termini. This suggests that glaciers in Porpoise Bay are very unlikely to calve with sea-ice present at their termini.

4.4 Atmospheric circulation anomalies

Atmospheric circulation anomalies in the months preceding the January 2007 and March 2016 sea-ice break-ups reveal contrasting conditions. In the austral summer which preceded the January 2007 break-up there were strong atmospheric anomalies throughout December 2005 (Fig. 9a). During December 2005 there was an anomalous easterly airflow adjacent to Porpoise Bay, which likely represents the weakening of the westerly winds which encircle Antarctica. This is reflected in the band of cooler SST close to the coast which represents the northward shift of the Antarctic Coastal Current in response to the weakened westerlies (e.g. Langlais et al., 2015). A weakened zonal flow combined with high sea surface temperatures (SST) in the south Pacific would allow the advection of warmer maritime air into Porpoise Bay. Consistent with this are the estimates of exceptionally high RACMO2.3 derived melt values in Porpoise Bay during December 2005, which contrasts with the longer term trend of cooling (Fig. 10). However this anomaly was short lived and, by January 2006, the wind field was close to average, although SST remained slightly higher than average (Fig. 9b). In December and January 2006/07, which are the months immediately before and during the break-up of sea-ice, atmosphere anomalies were close to average, with very little deviation from mean conditions in the wind field and a small negative SST anomaly (Fig. 9c). However, on January 11th 2007, which is the estimated date of sea-ice break-up, we note that there was a wind event close to Porpoise Bay (Fig. 11a).

In contrast to the preceding months to the January 2007 event, we find little deviations from average conditions prior to the March 2016 break-up event. In the austral summer which preceded the 2016 breakout (2014/15), there was little deviation from the average wind field and a small increase from average SST (Fig 9d). In December and January 2015/16 there was evidence for a small increase in the strength of westerly winds, and cooler SSTs in the South Pacific (Fig. 9e). However, in February and March 2016 there was no change from the average wind field and slightly cooler SST (Fig. 9f), although we note that on March 19th 2016, the estimated date of break-up initiation, there was a low pressure system passing Porpoise Bay (Fig. 11b).

4.6 Holmes (West) Glacier calving cycle

Through mapping the terminus position in all available satellite imagery (Table 1) dating back to 1963, we are able to reconstruct large calving events on the largest glacier in Porpoise bay, Holmes (West) (Fig. 12). On the basis that a large calving event is likely during the largest sea-ice break-up events, we estimate the date of calving based on sea-ice concentrations in Porpoise Bay when satellite imagery is not available. Our estimates suggest that Holmes (West) Glacier calves at approximately the same position in each calving cycle, including the most recent calving event in March 2016.

5. Discussion

5.1 Sea-ice break-up and the disintegration of glacier tongues in Porpoise Bay

We report a major, near-synchronous calving event in January 2007 and a similar event that was initiated in 2016 and resulted in $\sim 2,900 \text{ km}^2$ and $2,200 \text{ km}^2$ of ice, respectively, being removed from glacier tongues in the Porpoise Bay region of East Antarctica. This is comparable to some of the largest disintegration events ever observed in Antarctica e.g. Larsen A in 1995 ($4,200 \text{ km}^2$) and Larsen B in 2002 ($3,250 \text{ km}^2$); and is the largest event to have been observed in East Antarctica. However, this event differs to those observed on the ice shelves of the Antarctic Peninsula, in that it may be more closely linked to a cycle of glacier advance and retreat, as opposed to a catastrophic collapse that may be unprecedented.

Given the correspondence between the sea-ice and glacier terminus changes, we suggest that these disintegration events were driven by the break-up of the multi-year land-fast sea-ice which usually occupies Porpoise Bay and the subsequent loss of buttressing of the glacier termini. A somewhat similar mechanism has been widely documented in Greenland, where the dynamics of sea-ice melange in proglacial fjords has been linked to inter-annual variations in glacier terminus position (Amundson et al., 2010; Carr et al., 2013; Todd and Christoffersen, 2014; Cassotto et al., 2015). Additionally, the mechanical coupling between thick multi-year landfast sea ice and glacier tongues may have acted to stabilize and delay the calving of the Mertz glacier tongue (Massom et al., 2010) and Brunt/Stancomb-Wills Ice Shelf system (Khazendar et al., 2009). However, this is the first observational evidence directly linking multi-year landfast sea-ice break-up to the large scale and rapid disintegration of glacier tongues. This is important because landfast sea-ice is highly sensitive to climate (Heil, 2006; Mahoney et al., 2007) and, if future changes in climate were to result in a change to the persistence and/or stability of the landfast ice in Porpoise Bay, it may result in detrimental

283 effects on glacier tongue stability. An important question, therefore, is: what process(es) cause
284 sea-ice break-up?

285 **5.2 What caused the January 2007 and March 2016 sea-ice break-ups?**

286 The majority of sea-ice in Porpoise Bay is multi-year sea-ice (Fraser et al., 2012), and it is
287 likely that multiple climatic processes operating over different timescales contributed to the
288 January 2007 sea-ice break-up event. Although there are no long-term observations of multi-
289 year sea-ice thickness in Porpoise Bay, observations and models of the annual cycle of multi-
290 year sea-ice in other regions of East Antarctica suggest that multi-year sea-ice thickens
291 seasonally and thins each year (Lei et al., 2010; Sugimoto et al., 2016; Yang et al., 2016).
292 Therefore, the relative strength, stability and thickness of multi-year sea ice at a given time
293 period is driven not only by synoptic conditions in the short term (days/weeks), but also by
294 climatic conditions in the preceding years.

295 In the austral summer (2005/06) which preceded the break-up event in January 2007, there was
296 a strong easterly airflow anomaly throughout December 2005 directly adjacent to Porpoise Bay
297 (Fig. 9a). This anomaly represents the weakening of the band of westerly winds which encircle
298 Antarctica, which is reflected in an exceptionally negative Southern Annular Mode (SAM)
299 index in December 2005 (Marshall, 2003), and which contrasts with the long-term trend for a
300 positive SAM index (Marshall, 2007; Miles et al., 2013). A weaker band of westerly winds
301 combined with anomalously high SST in the Southern Pacific (Fig. 9a) would allow a greater
302 advection of warmer maritime air towards Porpoise Bay. Indeed, RACMO2.3 derived surface
303 melt estimates place December 2005 as the second highest mean melt month (1979-2015) on
304 the modelled output in Porpoise Bay (Fig. 10). To place this month into perspective, we note
305 that it would rank above the average melt values of all Decembers and Januarys since 2000 on
306 the remnants of Larsen B ice shelf. Comparing MODIS satellite imagery from before and after
307 December 2005 reveals the development of significant fracturing in the multi-year sea-ice (Fig
308 13a, b). These same fractures are still visible prior to the break-out event in January 2007 and,
309 when the multi-year sea-ice begins to break-up, it ruptures along these pre-existing weaknesses
310 (Fig. 13c). Therefore, this strongly suggests that the atmospheric circulation anomalies of
311 December 2005 played an important role in the January 2007 multi-year sea-ice break-up and
312 near-simultaneous calving event.

313 The break-up of Landfast sea-ice has been linked to dynamic wind events and ocean swell
314 (Heil, 2006; Ushio, 2006; Fraser et al., 2012). Therefore, it is possible that the wind anomalies

315 in December 2005 may have been important in initiating the fractures observed in the sea-ice
316 in Porpoise Bay, through changing the direction and/or intensity of oceanic swell. However,
317 this mechanism is thought to be at its most potent during anonymously low pack ice
318 concentrations because pack ice can act as a buffer to any oceanic swell (Langhorne et al.,
319 2001; Heil, 2006; Fraser, 2012). That said, we note that pack ice concentrations offshore of
320 Porpoise Bay were around average during December 2005 (Fig. 7). This may suggest that there
321 are other mechanisms that were important in the weakening of the multi-year sea-ice in
322 Porpoise Bay in December 2005.

323 In the Arctic, sea-ice melt ponding along pre-existing weaknesses has been widely reported to
324 precede sea-ice break-up (Ehn et al., 2011; Petrich et al., 2012; Landy et al., 2014; Schroder et
325 al., 2014; Arntsen et al., 2015). Despite its importance in the Arctic, it has yet to be considered
326 as a possible factor in landfast sea-ice break-up in coastal Antarctica. As a consequence of the
327 high melt throughout December 2005, the growth of sea-ice surface ponding would be
328 expected, in addition to surface thinning of the sea-ice. High-resolution cloud free optical
329 satellite coverage of Porpoise Bay throughout December 2005 is limited. However, available
330 ASTER imagery in the vicinity of Frost Glacier on the 4th and 31st December 2005 shows
331 surface melt features and the development of fractures throughout the month (Fig. 13 d and e)
332 and high resolution imagery from 16th January 2006 shows the development of melt ponds on
333 the sea-ice surface (Fig. 13 f). Therefore, we suggest it is possible that surface melt had some
334 impact on the fracturing of landfast sea-ice in Porpoise Bay. This may have been caused
335 through hydro-fracture of pre-existing depressions in the landfast ice or surface thinning
336 making it more vulnerable to fracture through ocean swell or internal stresses. Additionally,
337 the subsequent refreezing of some melt ponds may temporally inhibit basal ice growth,
338 potentially weakening the multi-year sea-ice for future break-up (Flocco et al., 2015).

339 Consistent with the notion that the multi-year sea-ice was already in a weakened state prior to
340 its break-up in 2007, is that the break-up occurred in January, several weeks before the likely
341 annual minimums in multi-year sea-ice thickness (Yang et al., 2016; Lei et al., 2010) and
342 landfast ice extent (Fraser et al., 2012). Additionally, atmospheric circulation anomalies
343 indicate little deviation from average conditions in the immediate months preceding break-up
344 (Fig. 9b, c), suggesting that atmospheric conditions were favourable for sea-ice stability.
345 Despite this, a synoptic event is still likely required to force the break-up in January 2007.
346 Daily sea-ice concentrations in Porpoise Bay in January 2007 show a sharp decrease in
347 sea-ice concentrations after 12th January, representing the onset of sea-ice break-out (Fig 14).

This is preceded by a strong melt event recorded by the RACMO2.3 model, centred on January 11th, which may represent a low pressure system. Indeed, ERA-interim estimates of the wind field suggest strong south-easterly winds in the vicinity of Porpoise Bay (Fig 11 a). Unlike in December 2005, pack ice concentrations offshore of Porpoise Bay were anomalously low (Fig. 7). Therefore, with less pack ice buttressing, it is possible that the melt event, high winds and associated ocean swell may have initiated the break-up of the already weakened multi-year sea-ice in Porpoise Bay.

In contrast to January 2007, we find no link between atmospheric circulation anomalies and the March 2016 sea-ice break-up. In the preceding months to the March 2016 break-up, wind and SST anomalies indicate conditions close to average conditions favouring sea-ice stability (Fig. 9 d, e, f). This suggests another process was important in driving the March 2016 sea-ice break-up. A key difference between the 2007 and 2016 event is that the largest glacier in the bay, Holmes (West), only calved in the 2016 event. Analysis of its calving cycle (Fig. 12) indicates that it calves at roughly the same position in each cycle and that its relative position in early 2016 suggests that calving was ‘overdue’ (Fig. 12). This indicates that the calving cycle of Holmes (West) Glacier is not necessarily driven by atmospheric circulation anomalies. Instead, we suggest that as Holmes (West) Glacier advances, it slowly pushes the multi-year sea-ice attached to its terminus further towards the open ocean to the point where the sea-ice attached to the glacier tongue becomes more unstable. This could be influenced by local bathymetry and oceanic circulation, but no observations are available. However, once the multi-year sea-ice reaches an unstable state, break-up is still likely to be forced by a synoptic event. This is consistent with our observations, where ERA-interim derived wind fields show the presence of a low pressure system close to Porpoise Bay on the estimated date of sea-ice break-up in March 2016 (Fig. 11 b). Whilst we suggest that the March 2016 sea-ice break-up and subsequent calving of Holmes (West) is currently part of a predictable cycle, we note that this could be vulnerable to change if any future changes in climate alter the persistence and/or strength of the multi-year sea-ice, which is usually attached to the glacier terminus.

6. Conclusion

We identify two large near-simultaneous calving events in January 2007 and March 2016 which were driven by the break-up of the multi-year landfast sea-ice which usually occupies the bay. This provides a previously unreported mechanism for the rapid disintegration of

floating glacier tongues in East Antarctica, adding to the growing body of research linking glacier tongue stability to the mechanical coupling of landfast ice (e.g. Khazander et al., 2009; Massom et al., 2010). Our results suggest that multi-year sea-ice break-ups in 2007 and 2016 in Porpoise Bay were driven by different mechanisms. We link the 2007 event to atmospheric circulation anomalies in December 2005 weakening multi-year sea-ice through a combination of surface melt and a change in wind direction, prior to its eventual break-up in 2007. This is in contrast to the March 2016 event, which we suggest is part of a longer-term cycle based on the terminus position of Holmes (West) Glacier that was able to advance and push sea-ice out of the bay. The link between sea-ice break-up and major calving of glacier tongues is especially important because it suggests predictions of future warming (DeConto and Pollard, 2016) suggests that multi-year landfast ice may become less persistent. Therefore, the glacier tongues which depend on landfast ice for stability may become less stable in the future. In a wider context, our results also highlight the complex nature of the mechanisms which drive glacier calving position in Antarctica. Whilst regional trends in terminus position can be driven by ocean-climate-sea-ice interaction (e.g. Miles et al., 2013; 2016), individual glaciers and individual calving events have the potential respond differently to similar climatic forcing.

Acknowledgements: We thank the ESA for providing Envisat ASAR WSM data (Project ID: 16713) and Sentinel data. Landsat imagery was provided free of charge by the U.S. Geological Survey Earth Resources Observation Science Centre. We thank M. van den Broeke for providing data and assisting with RACMO. B.W.J.M was funded by a Durham University Doctoral Scholarship program. S.S.R.J. was supported by Natural Environment Research Council Fellowship NE/J018333/1. We thank two reviewers and the Editor for comments that lead to substantial improvement of this manuscript.

410 **References**

- 411 Aitken, A. R. A., Roberts, J. L., van Ommen, T. D., Young, D. A., Golledge, N. R.,
 412 Greenbaum, J. S., Blankenship, D. D., and Siegert, M. J.: Repeated large-scale retreat and
 413 advance of Totten Glacier indicated by inland bed erosion, *Nature*, 533, 385-+,
 414 10.1038/nature17447, 2016.
- 415 Amundson, J. M., Fahnestock, M., Truffer, M., Brown, J., Luthi, M. P., and Motyka, R. J.: Ice
 416 melange dynamics and implications for terminus stability, Jakobshavn Isbrae Greenland, *J*
 417 *Geophys Res-Earth*, 115, Artn F01005 Doi 10.1029/2009jf001405, 2010.
- 418 Arntsen, A. E., Song, A. J., Perovich, D. K., and Richter-Menge, J. A.: Observations of the
 419 summer breakup of an Arctic sea ice cover, *Geophys Res Lett*, 42, 8057-8063,
 420 10.1002/2015GL065224, 2015.
- 421 Astrom, J. A., Vallot, D., Schafer, M., Welty, E. Z., O'Neel, S., Bartholomaeus, T. C., Liu, Y.,
 422 Riikila, T. I., Zwinger, T., Timonen, J., and Moore, J. C.: Termini of calving glaciers as self-
 423 organized critical systems, *Nat Geosci*, 7, 874-878, 10.1038/NGEO2290, 2014.
- 424 Banwell, A. F., MacAyeal, D. R., and Sergienko, O. V.: Breakup of the Larsen B Ice Shelf
 425 triggered by chain reaction drainage of supraglacial lakes, *Geophys Res Lett*, 40, 5872-5876,
 426 10.1002/2013GL057694, 2013.
- 427 Bassis, J. N., and Jacobs, S.: Diverse calving patterns linked to glacier geometry, *Nat Geosci*,
 428 6, 833-836, 10.1038/NGEO1887, 2013.
- 429 Benn, D. I., Warren, C. R., and Mottram, R. H.: Calving processes and the dynamics of calving
 430 glaciers, *Earth-Sci Rev*, 82, 143-179, 10.1016/j.earscirev.2007.02.002, 2007.
- 431 Cassotto, R., Fahnestock, M., Amundson, J. M., Truffer, M., and Joughin, I.: Seasonal and
 432 interannual variations in ice melange and its impact on terminus stability, Jakobshavn Isbrae,
 433 Greenland, *J Glaciol*, 61, 76-88, 10.3189/2015JoG13J235, 2015.
- 434 Chapuis, A., and Tetzlaff, T.: The variability of tidewater-glacier calving: origin of event-size
 435 and interval distributions, *J Glaciol*, 60, 622-634, 10.3189/2014JoG13J215, 2014.
- 436 Comiso, J. C.: Bootstrap Sea Ice Concentrations from Nimbus-7 SMMR and DMSP SSM/I-
 437 SSMIS. Version 2, Boulder, Colorado USA: NASA National Snow and Ice Data Center
 438 Distributed Active Archive Center., 2014.
- 439 Cook, A. J., Fox, A. J., Vaughan, D. G., and Ferrigno, J. G.: Retreating Glacier Fronts on the
 440 Antarctic Peninsula over the Past Half-Century, *Science*, 308, 541-544,
 441 10.1126/science.1104235, 2005.
- 442 Cook, C. P., Hill, D. J., van de Flierdt, T., Williams, T., Hemming, S. R., Dolan, A. M., Pierce,
 443 E. L., Escutia, C., Harwood, D., Cortese, G., and Gonzales, J. J.: Sea surface temperature
 444 control on the distribution of far-traveled Southern Ocean ice-rafted detritus during the
 445 Pliocene, *Paleoceanography*, 29, 533-548, Doi 10.1002/2014pa002625, 2014.
- 446 De Angelis, H., and Skvarca, P.: Glacier surge after ice shelf collapse, *Science*, 299, 1560-
 447 1562, DOI 10.1126/science.1077987, 2003.

448 DeConto, R. M., and Pollard, D.: Contribution of Antarctica to past and future sea-level rise,
 449 Nature, 531, 591-+, 10.1038/nature17145, 2016.

450 Depoorter, M. A., Bamber, J. L., Griggs, J. A., Lenaerts, J. T. M., Ligtenberg, S. R. M., van
 451 den Broeke, M. R., and Moholdt, G.: Calving fluxes and basal melt rates of Antarctic ice
 452 shelves, Nature, 502, 89-+, Doi 10.1038/Nature12567, 2013.

453 Ehn, J. K., Mundy, C. J., Barber, D. G., Hop, H., Rossnagel, A., and Stewart, J.: Impact of
 454 horizontal spreading on light propagation in melt pond covered seasonal sea ice in the
 455 Canadian Arctic, J Geophys Res-Oceans, 116, Artn C00g02 10.1029/2010jc006908, 2011.

456 Flocco, D., Feltham, D. L., Bailey, E., and Schroeder, D.: The refreezing of melt ponds on
 457 Arctic sea ice, J Geophys Res-Oceans, 120, 647-659, 10.1002/2014JC010140, 2015.

458 Fraser, A. D., Massom, R. A., Michael, K. J., Galton-Fenzi, B. K., and Lieser, J. L.: East
 459 Antarctic Landfast Sea Ice Distribution and Variability, 2000-08, J Climate, 25, 1137-1156,
 460 10.1175/Jcli-D-10-05032.1, 2012.

461 Frezzotti, M., and Polizzi, M.: 50 years of ice-front changes between the Adelie and Banzare
 462 Coasts, East Antarctica, Ann Glaciol, 34, 235-240, 10.3189/172756402781817897, 2002.

463 Greenbaum, J. S., Blankenship, D. D., Young, D. A., Richter, T. G., Roberts, J. L., Aitken, A.
 464 R. A., Legresy, B., Schroeder, D. M., Warner, R. C., van Ommen, T. D., and Siegert, M. J.:
 465 Ocean access to a cavity beneath Totten Glacier in East Antarctica, Nat Geosci, 8, 294-298,
 466 10.1038/NGEO2388, 2015.

467 Heil, P.: Atmospheric conditions and fast ice at Davis, East Antarctica: A case study, J
 468 Geophys Res-Oceans, 111, Artn C05009 10.1029/2005jc002904, 2006.

469 Khazendar, A., Rignot, E., and Larour, E.: Roles of marine ice, rheology, and fracture in the
 470 flow and stability of the Brunt/Stancomb-Wills Ice Shelf, J Geophys Res-Earth, 114, Artn
 471 F04007 10.1029/2008jf001124, 2009.

472 Kim, K., Jezek, K. C., and Liu, H.: Orthorectified image mosaic of Antarctica from 1963
 473 Argon satellite photography: image processing and glaciological applications, Int J Remote
 474 Sens, 28, 5357-5373, 2007.

475 King, M. A., Bingham, R. J., Moore, P., Whitehouse, P. L., Bentley, M. J., and Milne, G. A.:
 476 Lower satellite-gravimetry estimates of Antarctic sea-level contribution, Nature, 491, 586-+,
 477 Doi 10.1038/Nature11621, 2012.

478 Landy, J., Ehn, J., Shields, M., and Barber, D.: Surface and melt pond evolution on landfast
 479 first-year sea ice in the Canadian Arctic Archipelago, J Geophys Res-Oceans, 119, 3054-3075,
 480 10.1002/2013JC009617, 2014.

481 Langhorne, P. J., Squire, V. A., Fox, C., and Haskell, T. G.: Lifetime estimation for a land-fast
 482 ice sheet subjected to ocean swell, Annals of Glaciology, Vol 33, 33, 333-338, Doi
 483 10.3189/172756401781818419, 2001.

484 Langlais, C. E., Rintoul, S. R., and Zika, J. D.: Sensitivity of Antarctic Circumpolar Current
 485 Transport and Eddy Activity to Wind Patterns in the Southern Ocean, J Phys Oceanogr, 45,
 486 1051-1067, 10.1175/Jpo-D-14-0053.1, 2015.

487 Lei, R. B., Li, Z. J., Cheng, B., Zhang, Z. H., and Heil, P.: Annual cycle of landfast sea ice in
 488 Prydz Bay, east Antarctica, *J Geophys Res-Oceans*, 115, Artn C02006 10.1029/2008jc005223,
 489 2010.

490 Liu, H. X., and Jezek, K. C.: A complete high-resolution coastline of antarctica extracted from
 491 orthorectified Radarsat SAR imagery, *Photogramm Eng Rem S*, 70, 605-616, 2004.

492 Mahoney, A., Eicken, H., Gaylord, A. G., and Shapiro, L.: Alaska landfast sea ice: Links with
 493 bathymetry and atmospheric circulation, *J Geophys Res-Oceans*, 112, Artn C02001
 494 10.1029/2006jc003559, 2007.

495 Marshall, G. J.: Trends in the southern annular mode from observations and reanalyses, *J*
 496 *Climate*, 16, 4134-4143, Doi 10.1175/1520-0442(2003)016<4134:Titsam>2.0.Co;2, 2003.

497 Marshall, G. J.: Half-century seasonal relationships between the Southern Annular Mode and
 498 Antarctic temperatures, *Int J Climatol*, 27, 373-383, 10.1002/joc.1407, 2007.

499 Massom, R. A., Giles, A. B., Warner, R. C., Fricker, H. A., Legresy, B., Hyland, G.,
 500 Lescarmonier, L., and Young, N.: External influences on the Mertz Glacier Tongue (East
 501 Antarctica) in the decade leading up to its calving in 2010, *J Geophys Res-Earth*, 120, 490-506,
 502 10.1002/2014JF003223, 2015.

503 McMillan, M., Shepherd, A., Sundal, A., Briggs, K., Muir, A., Ridout, A., Hogg, A., and
 504 Wingham, D.: Increased ice losses from Antarctica detected by CryoSat-2, *Geophys Res Lett*,
 505 41, 3899-3905, Doi 10.1002/2014gl060111, 2014.

506 Miles, B. W. J., Stokes, C. R., Vieli, A., and Cox, N. J.: Rapid, climate-driven changes in
 507 outlet glaciers on the Pacific coast of East Antarctica, *Nature*, 500, 563-+, Doi
 508 10.1038/Nature12382, 2013.

509 Miles, B. W. J., Stokes, C. R., and Jamieson, S. S. R.: Pan-ice-sheet glacier terminus change in
 510 East Antarctica reveals sensitivity of Wilkes Land to sea-ice changes, *Science Advances*, 2,
 511 10.1126/sciadv.1501350, 2016.

512 Moon, T., and Joughin, I.: Changes in ice front position on Greenland's outlet glaciers from
 513 1992 to 2007, *J Geophys Res-Earth*, 113, Artn F02022 Doi 10.1029/2007jf000927, 2008.

514 Parkinson, C. L., J. C. Comiso, and H. J. Zwally. 1999, updated 2004. *Nimbus-5 ESMR Polar*
 515 *Gridded Sea Ice Concentrations*. Edited by W. Meier and J. Stroeve. Boulder, Colorado USA:
 516 National Snow and Ice Data Center. Digital media.

517 Petrich, C., Eicken, H., Polashenski, C. M., Sturm, M., Harbeck, J. P., Perovich, D. K., and
 518 Finnegan, D. C.: Snow dunes: A controlling factor of melt pond distribution on Arctic sea ice,
 519 *J Geophys Res-Oceans*, 117, Artn C09029 10.1029/2012jc008192, 2012.

520 Pritchard, H. D., Arthern, R. J., Vaughan, D. G., and Edwards, L. A.: Extensive dynamic
 521 thinning on the margins of the Greenland and Antarctic ice sheets, *Nature*, 461, 971-975,
 522 10.1038/nature08471, 2009.

523 Rignot, E., Casassa, G., Gogineni, P., Krabill, W., Rivera, A., and Thomas, R.: Accelerated ice
 524 discharge from the Antarctic Peninsula following the collapse of Larsen B ice shelf, *Geophys*
 525 *Res Lett*, 31, Artn L18401 10.1029/2004gl020697, 2004.

526 Rignot, E., Mouginot, J., and Scheuchl, B.: Ice Flow of the Antarctic Ice Sheet, *Science*, 333,
527 1427-1430, 10.1126/science.1208336, 2011.

528 Rignot, E., Jacobs, S., Mouginot, J., and Scheuchl, B.: Ice-Shelf Melting Around Antarctica,
529 *Science*, 341, 266-270, DOI 10.1126/science.1235798, 2013.

530 Rott, H., Skvarca, P., and Nagler, T.: Rapid collapse of northern Larsen Ice Shelf, Antarctica,
531 *Science*, 271, 788-792, DOI 10.1126/science.271.5250.788, 1996.

532 Rott, H., Rack, W., Skvarca, P., and De Angelis, H.: Northern Larsen Ice Shelf, Antarctica:
533 further retreat after collapse, *Annals of Glaciology*, Vol 34, 2002, 34, 277-282, Doi
534 10.3189/172756402781817716, 2002.

535 Sasgen, I., Konrad, H., Ivins, E. R., Van den Broeke, M. R., Bamber, J. L., Martinec, Z., and
536 Klemann, V.: Antarctic ice-mass balance 2003 to 2012: regional reanalysis of GRACE satellite
537 gravimetry measurements with improved estimate of glacial-isostatic adjustment based on GPS
538 uplift rates, *Cryosphere*, 7, 1499-1512, DOI 10.5194/tc-7-1499-2013, 2013.

539 Scambos, T., Hulbe, C., and Fahnestock, M.: Climate-induced ice shelf disintegration in the
540 Antarctic Peninsula, *Antarct Res Ser*, 79, 79-92, 2003.

541 Scambos, T., Fricker, H. A., Liu, C. C., Bohlander, J., Fastook, J., Sargent, A., Massom, R.,
542 and Wu, A. M.: Ice shelf disintegration by plate bending and hydro-fracture: Satellite
543 observations and model results of the 2008 Wilkins ice shelf break-ups, *Earth Planet Sc Lett*,
544 280, 51-60, 10.1016/j.epsl.2008.12.027, 2009.

545 Schroder, D., Feltham, D. L., Flocco, D., and Tsamados, M.: September Arctic sea-ice
546 minimum predicted by spring melt-pond fraction, *Nat Clim Change*, 4, 353-357,
547 10.1038/Nclimate2203, 2014.

548 Spreen, G., Kaleschke, L., and Heygster, G.: Sea ice remote sensing using AMSR-E 89-GHz
549 channels, *J Geophys Res-Oceans*, 113, Artn C02s0310.1029/2005jc003384, 2008.

550 Sugimoto, F., Tamura, T., Shimoda, H., Uto, S., Simizu, D., Tateyama, K., Hoshino, S., Ozeki,
551 T., Fukamachi, Y., Ushio, S., and Ohshima, K. I.: Interannual variability in sea-ice thickness in
552 the pack-ice zone off Lutzow-Holm Bay, East Antarctica, *Polar Sci*, 10, 43-51,
553 10.1016/j.polar.2015.10.003, 2016.

554 Todd, J., and Christoffersen, P.: Are seasonal calving dynamics forced by buttressing from ice
555 melange or undercutting by melting? Outcomes from full-Stokes simulations of Store Glacier,
556 West Greenland, *Cryosphere*, 8, 2353-2365, 10.5194/tc-8-2353-2014, 2014.

557 Ushio, S.: Factors affecting fast-ice break-up frequency in Lutzow-Holm bay, Antarctica,
558 *Annals of Glaciology*, Vol 44, 2006, 44, 177-182, Doi 10.3189/172756406781811835, 2006.

559 van der Veen, C. J.: Calving glaciers, *Prog Phys Geog*, 26, 96-122,
560 10.1191/0309133302pp327ra, 2002.

561 van Wessem, J. M., Reijmer, C. H., Morlighem, M., Mouginot, J., Rignot, E., Medley, B.,
562 Joughin, I., Wouters, B., Depoorter, M. A., Bamber, J. L., Lenaerts, J. T. M., van de Berg, W.
563 J., van den Broeke, M. R., and van Meijgaard, E.: Improved representation of East Antarctic

564 surface mass balance in a regional atmospheric climate model, *J Glaciol*, 60, 761-770,
 565 10.3189/2014JoG14J051, 2014.

566 Wang, X., Holland, D. M., Cheng, X., and Gong, P.: Grounding and Calving Cycle of Mertz
 567 Ice Tongue Revealed by Shallow Mertz Bank, *The Cryosphere Discuss.*, 2016, 1-37,
 568 10.5194/tc-2016-3, 2016.

569 Wuite, J., Rott, H., Hetzenecker, M., Floricioiu, D., De Rydt, J., Gudmundsson, G. H., Nagler,
 570 T., and Kern, M.: Evolution of surface velocities and ice discharge of Larsen B outlet glaciers
 571 from 1995 to 2013, *Cryosphere*, 9, 957-969, 10.5194/tc-9-957-2015, 2015.

572 Yang, Y., Li, Z. J., Leppazranta, M., Cheng, B., Shi, L. Q., and Lei, R. B.: Modelling the
 573 thickness of landfast sea ice in Prydz Bay, East Antarctica, *Antarct Sci*, 28, 59-70,
 574 10.1017/S0954102015000449, 2016.

575 Young, D. A., Wright, A. P., Roberts, J. L., Warner, R. C., Young, N. W., Greenbaum, J. S.,
 576 Schroeder, D. M., Holt, J. W., Sugden, D. E., Blankenship, D. D., van Ommen, T. D., and
 577 Siegert, M. J.: A dynamic early East Antarctic Ice Sheet suggested by ice-covered fjord
 578 landscapes, *Nature*, 474, 72-75, 10.1038/nature10114, 2011.

579

580

581

582

583

584

585

586

587

588

589

590

591

592

593

594

595

Table 1: Satellite imagery used in the study

Satellite	Date of Imagery
ARGON	October 1963 (Kim et al., 2007)
Envisat ASAR WSM	August 2002, November 2002 to March 2012 (monthly)
Landsat	January 1973; February 1991
MODIS	January 2001; December/January 2005/6; March 2016
RADARSAT	September 1997 (Liu and Jezek, 2004)
Sentinel-1	February-July, 2016

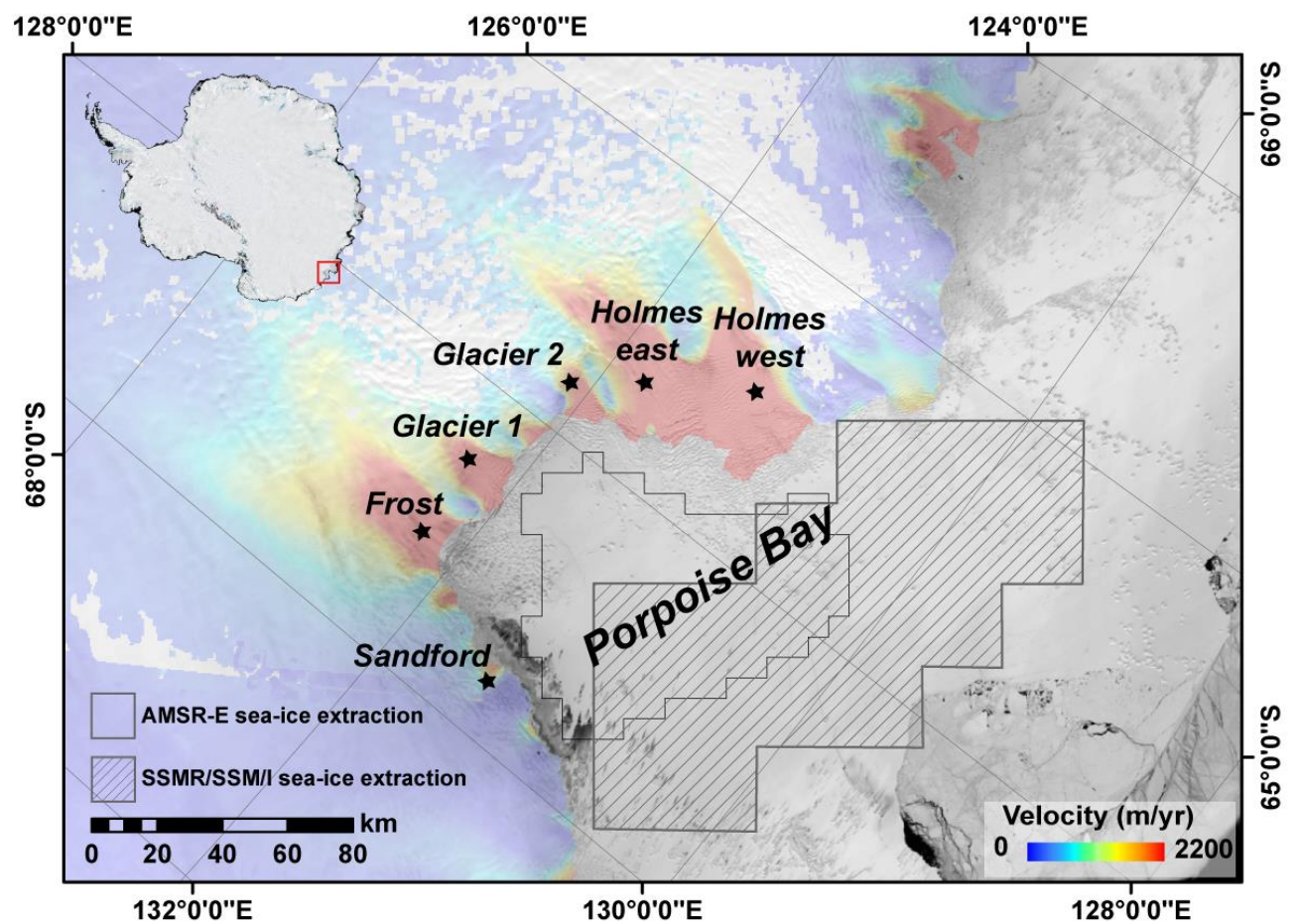


Figure 1: MODIS image of Porpoise Bay, with glacier velocities overlain (Rignot et al., 2011). The hatched polygon represents the region where long-term 25 km resolution SSMR/SSM/I sea-ice concentrations were extracted. The non-hatched polygon represents the region where the higher resolution (6.25 km) AMSR-E sea-ice concentrations were extracted.

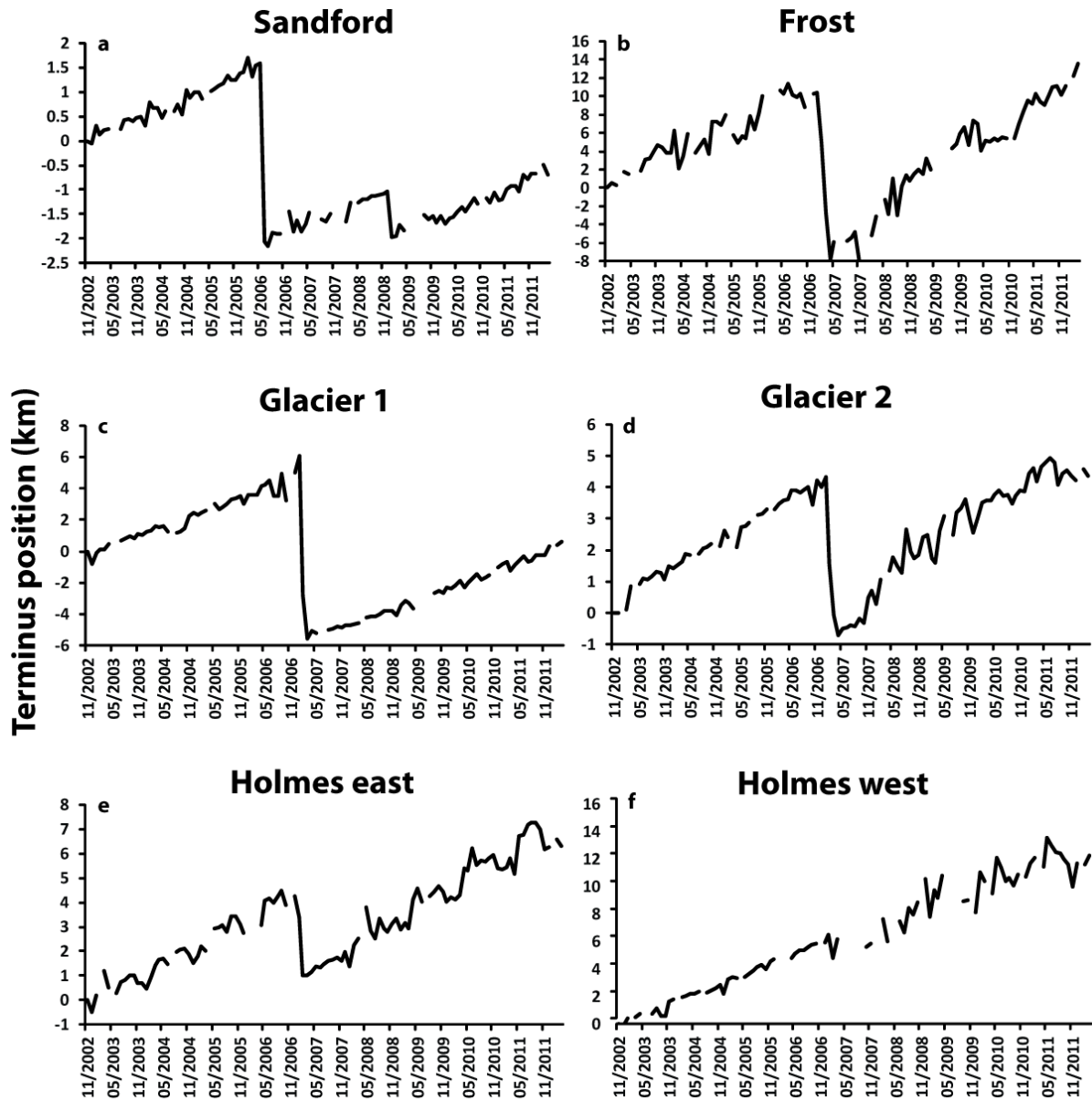


Figure 2: Terminus position change of six glaciers in porpoise Bay between November 2002 and March 2012. Note the major calving event in January 2007 for 5 of the glaciers. Terminus position measurements are subject to ± 500 m. Note the different scales on y-axis.

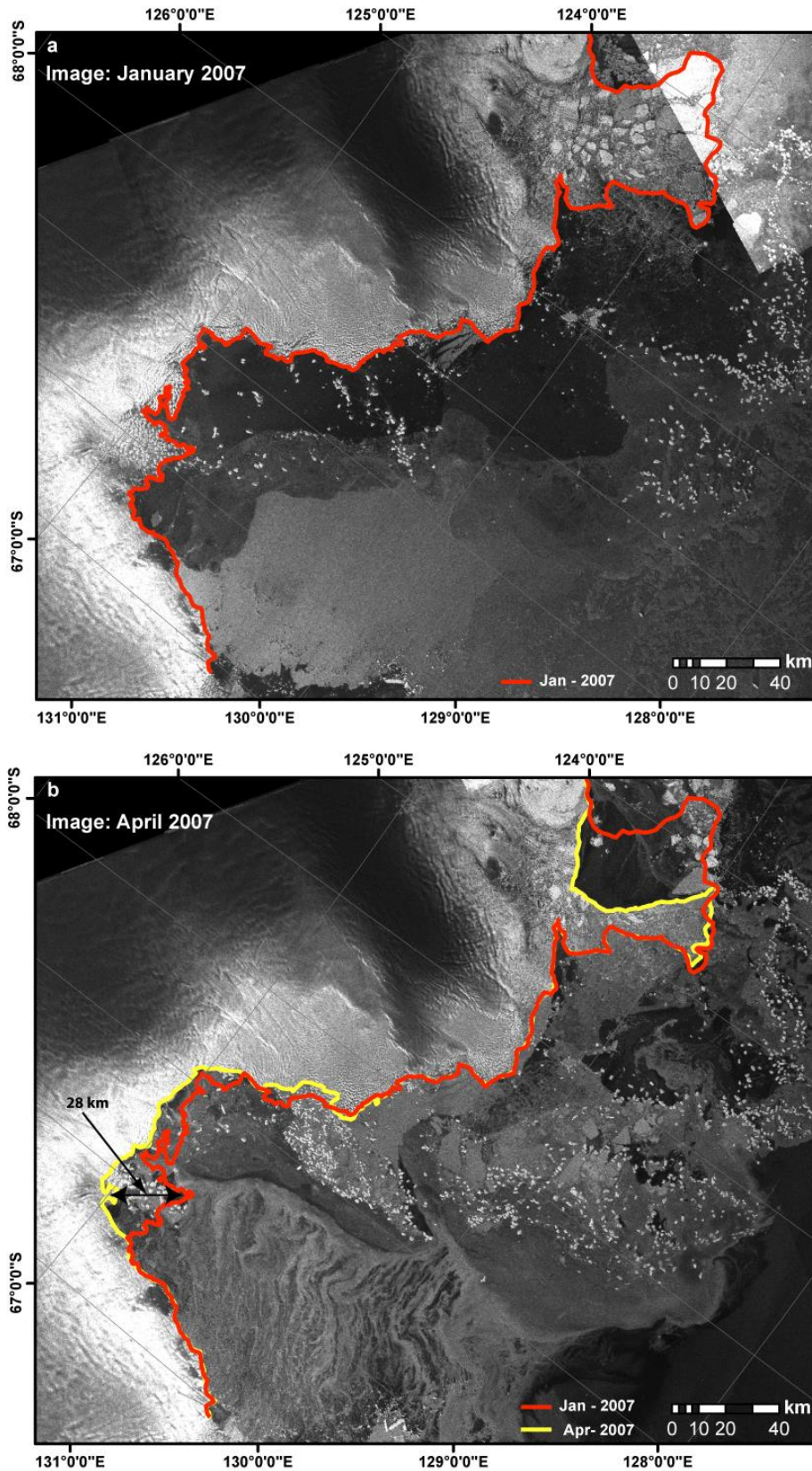


Figure 3: Envisat ASAR WSM imagery in January 2007 **a)** and April 2007 **b)**, which are immediately prior to and after a near-simultaneous calving event in Porpoise Bay. Red line shows terminus positions in January 2007 and yellow line shows the positions in April 2007.

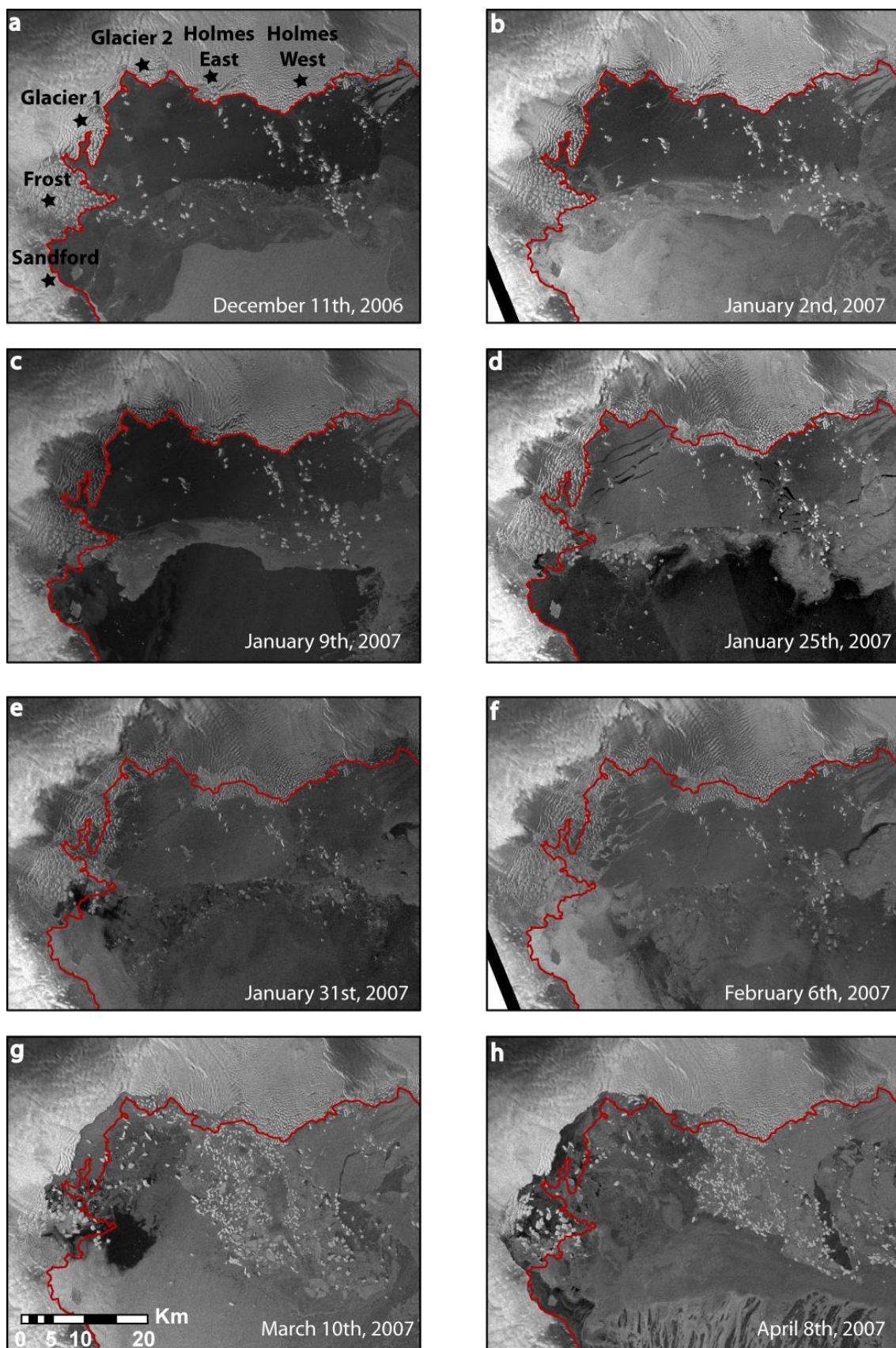


Figure 4: Envisat ASAR WSM imagery showing the evolution of the 2007 calving event. Red line shows the terminus positions from December 11th 2006 on all panels.

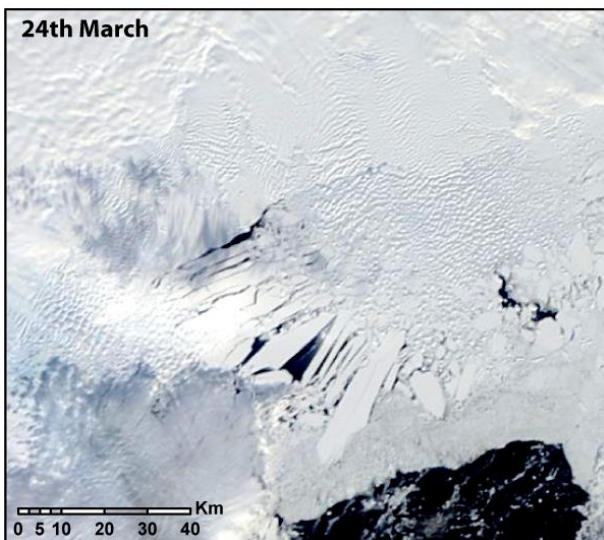
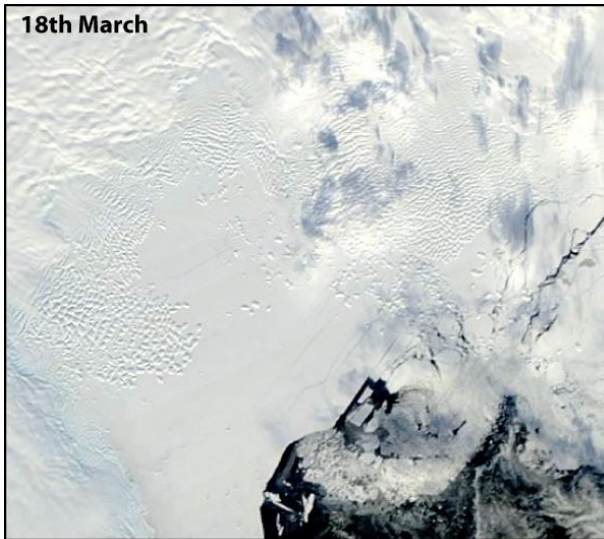
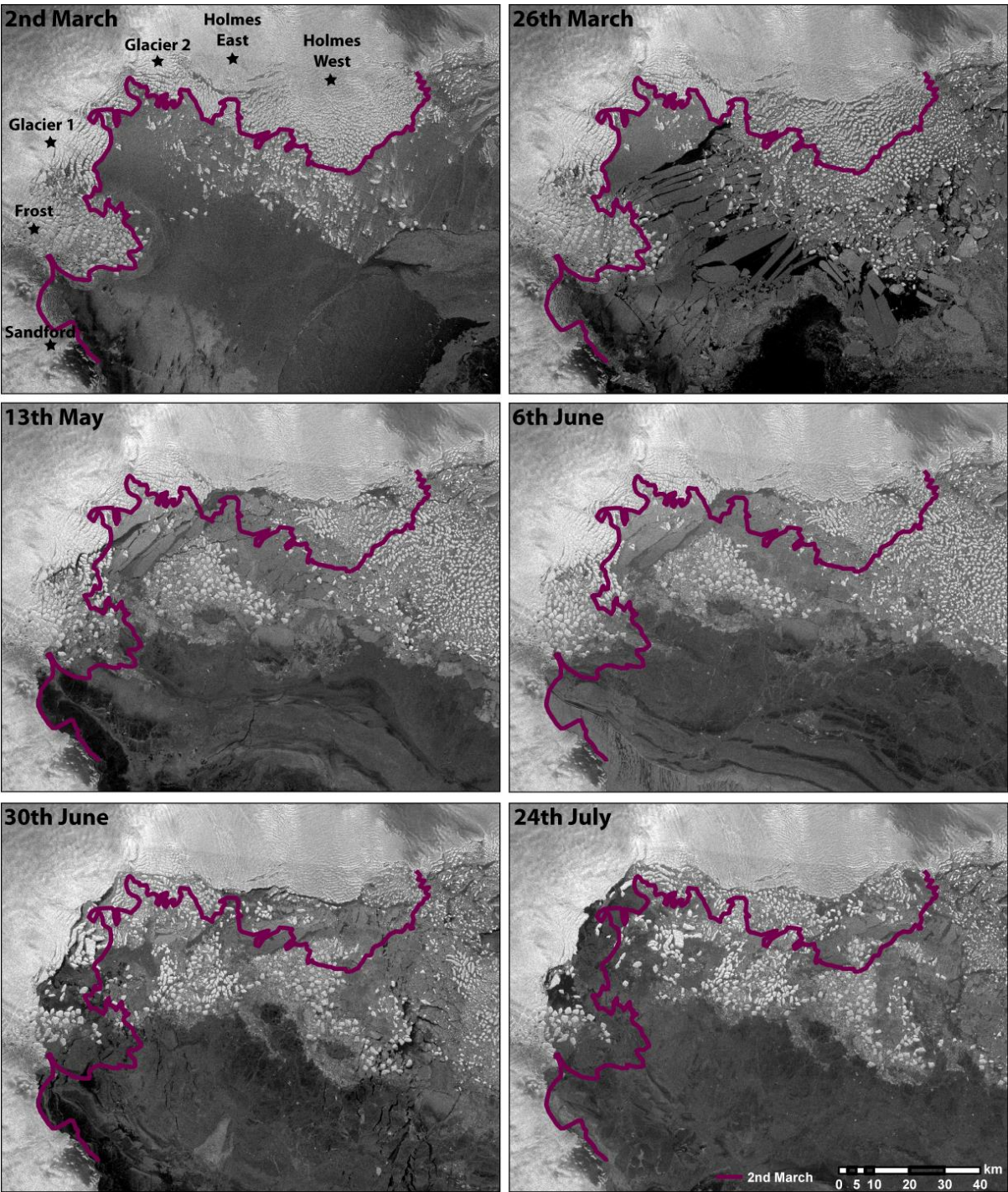


Figure 5: MODIS imagery showing the initial stages of disintegration of Holmes (West) Glacier in March 2016. On March 19th a large section of sea-ice breaks away from the terminus (circled), initiating the rapid disintegration process. By the 24th March an 800 km² section of Holmes (west) glacier tongue had disintegrated.



622

623 **Figure 6:** Sentinel-1 imagery showing the evolution of the 2016 calving event. Purple line
624 shows the terminus position from 2nd March on all panels.

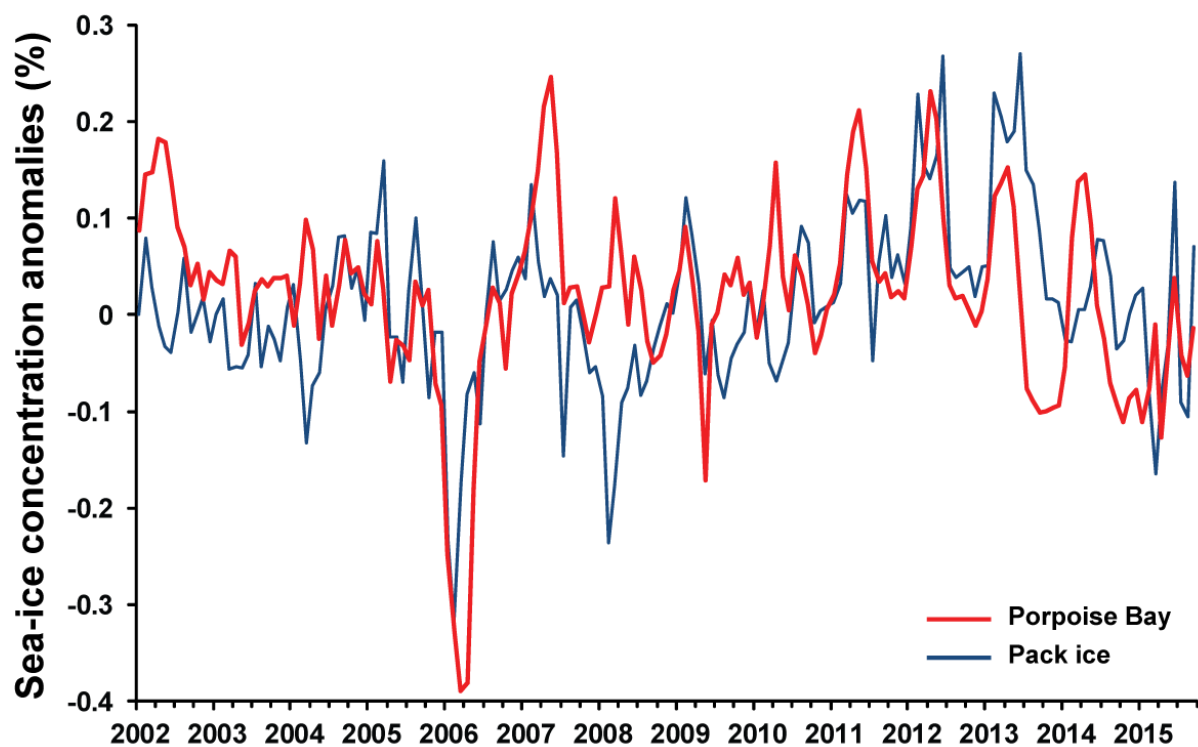


Fig 7: Mean monthly sea-ice concentration anomalies from November 2002 to June 2016. The red line indicates sea-ice concentration anomalies in Porpoise Bay and the blue line indicates pack ice concentration anomalies.

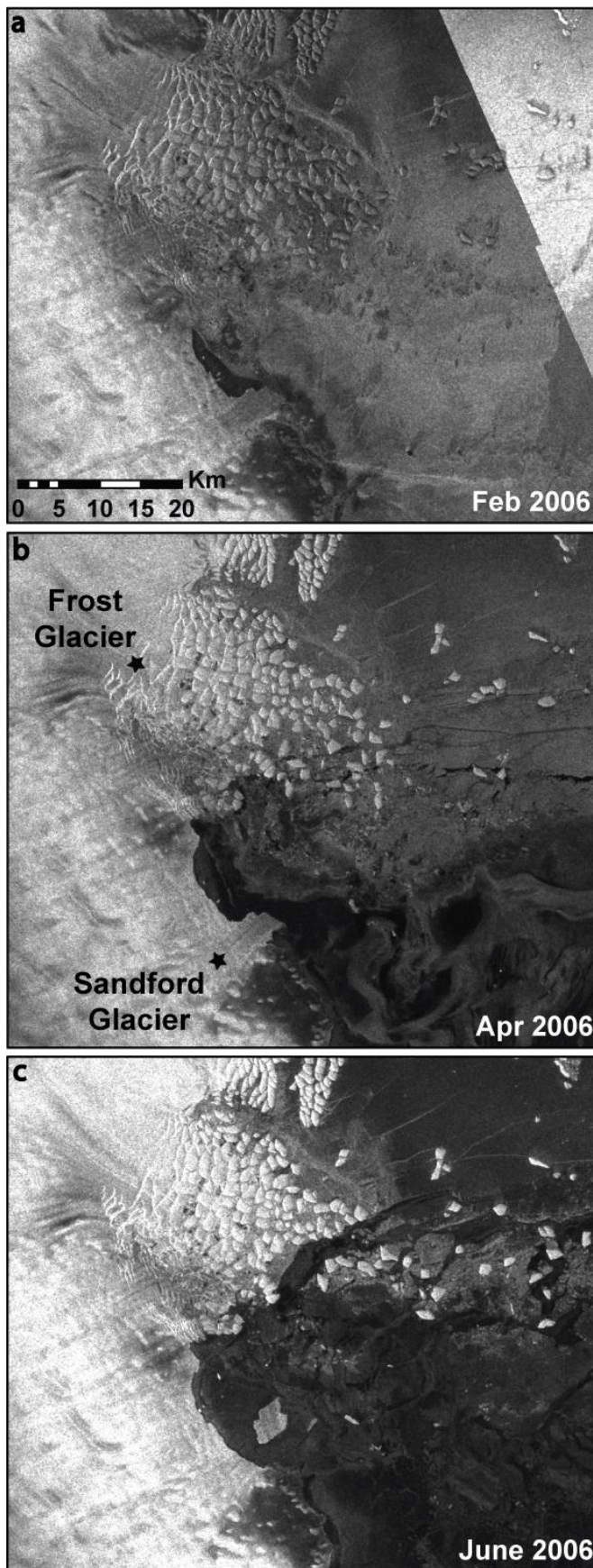


Figure 8: Time series of Frost and Sanford Glaciers calving showing that sea-ice clears prior to calving and dispersal of icebergs.

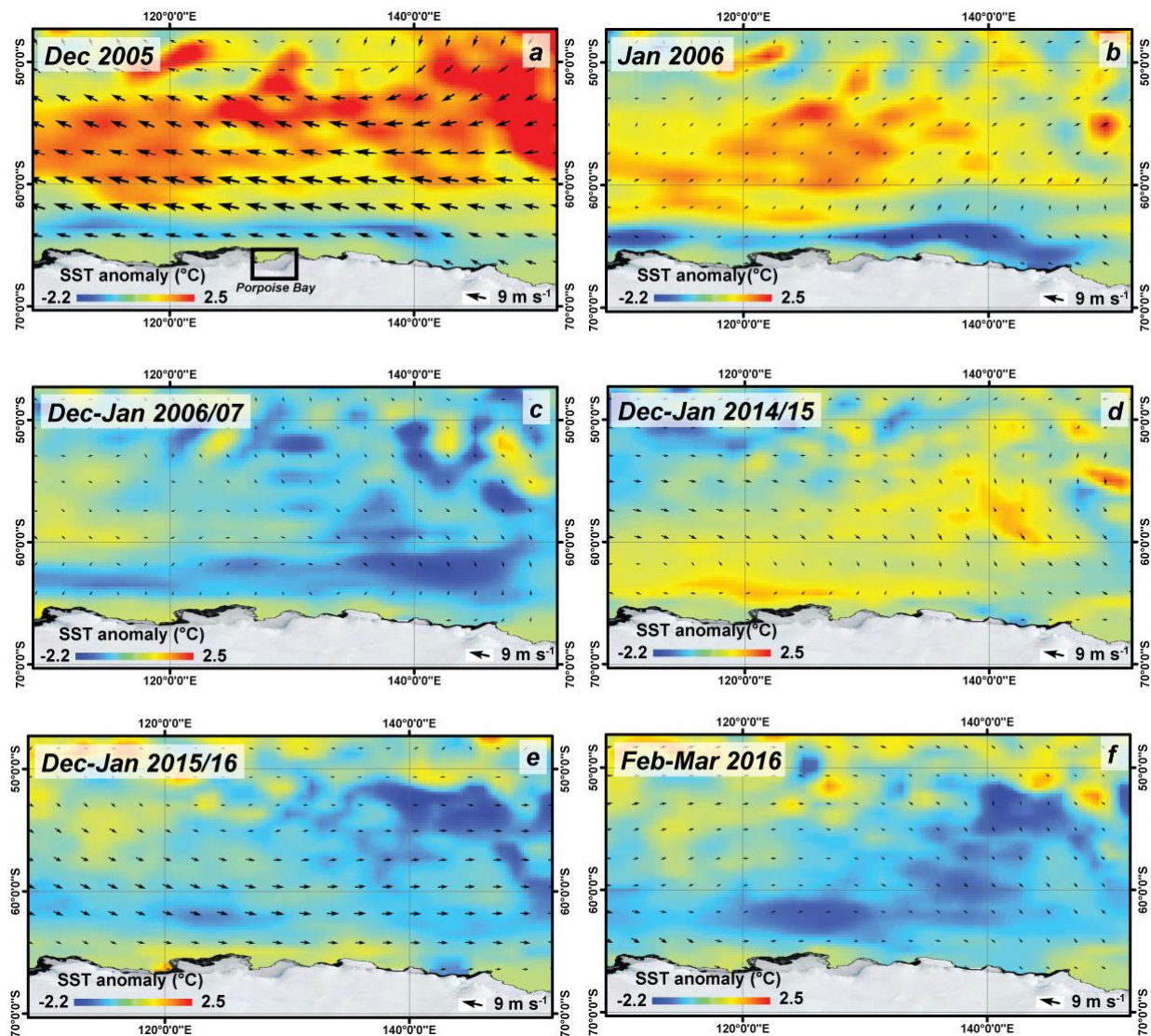


Figure 9: Mean monthly ERA-interim derived wind field and sea surface temperature anomalies in the months preceding the 2007 and 2016 sea-ice break-ups. **a)** December 2005 **b)** January 2006 **c)** Mean December and January 2006/07 **d)** Mean December and January 2014/15 **e)** Mean December and January 2015/16 **f)** Mean February and March 2016.

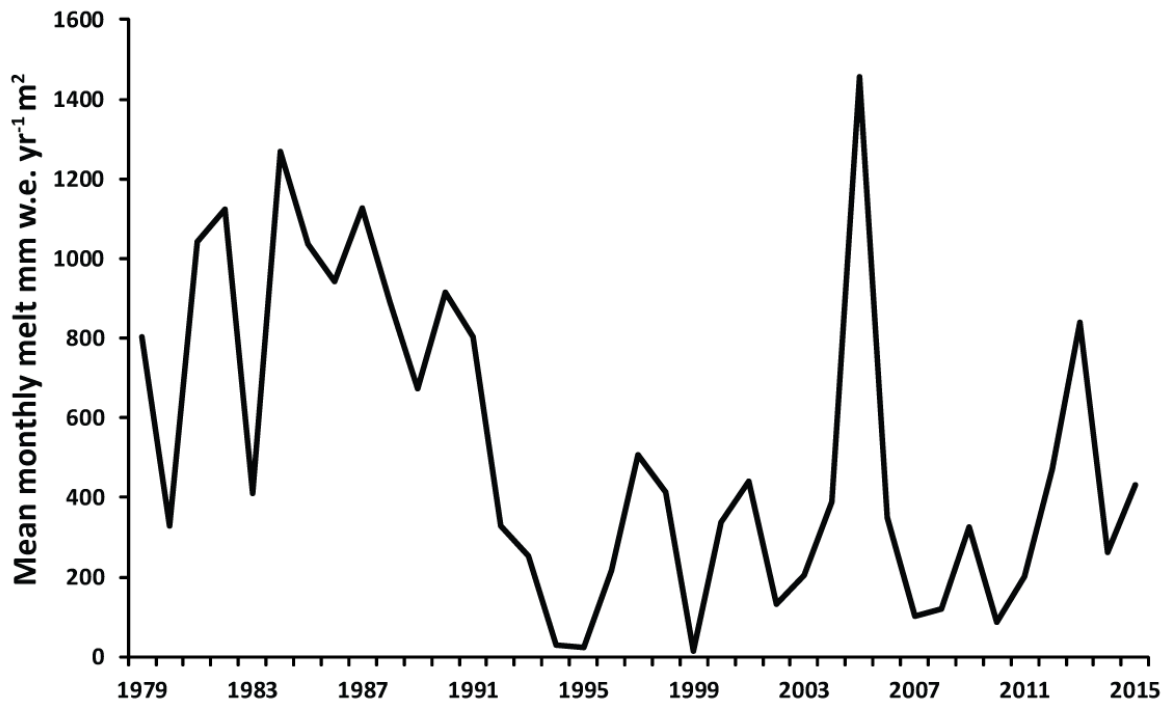


Figure 10: Mean RACMO2.3 derived December melt 1979-2015 in Porpoise Bay.

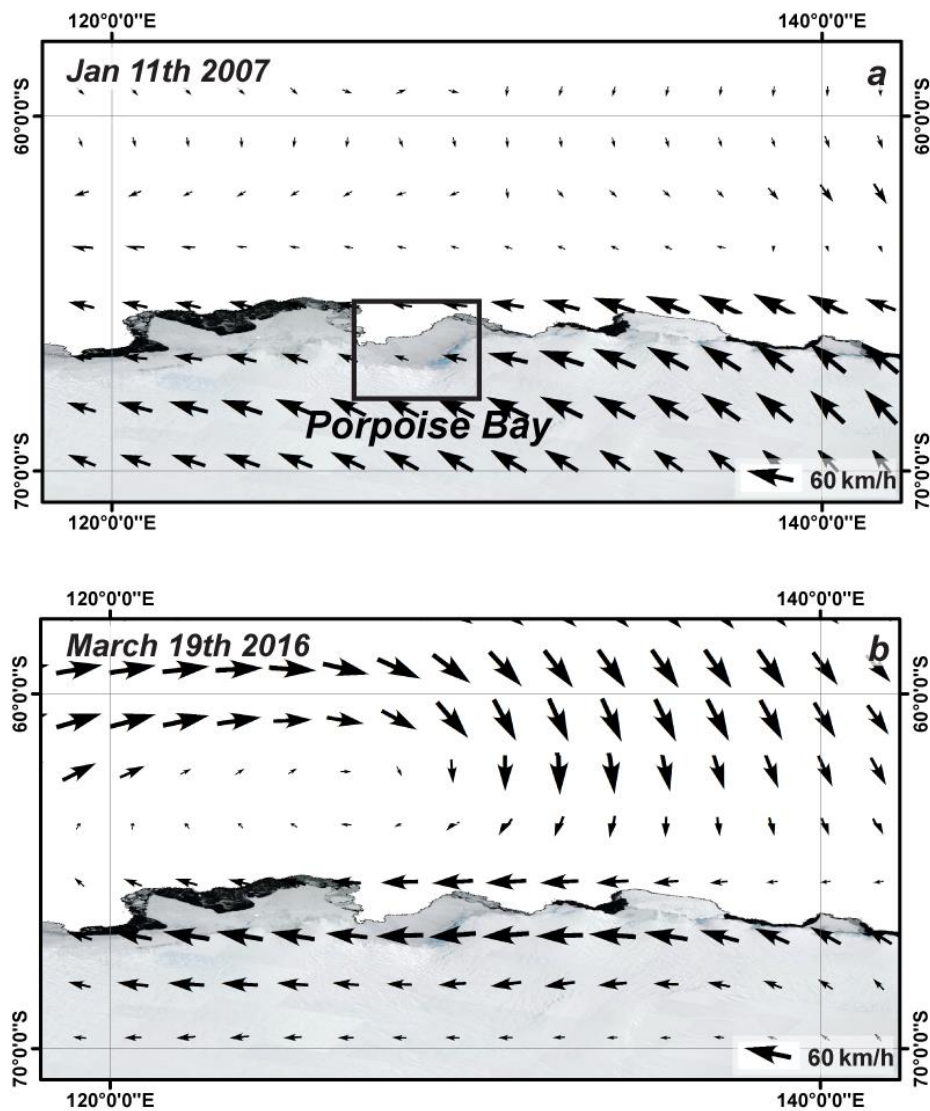


Figure 11: ERA-interim derived wind fields for the estimated dates of sea-ice break-up. **a)** January 11th 2007 and **b)** March 19th 2016.

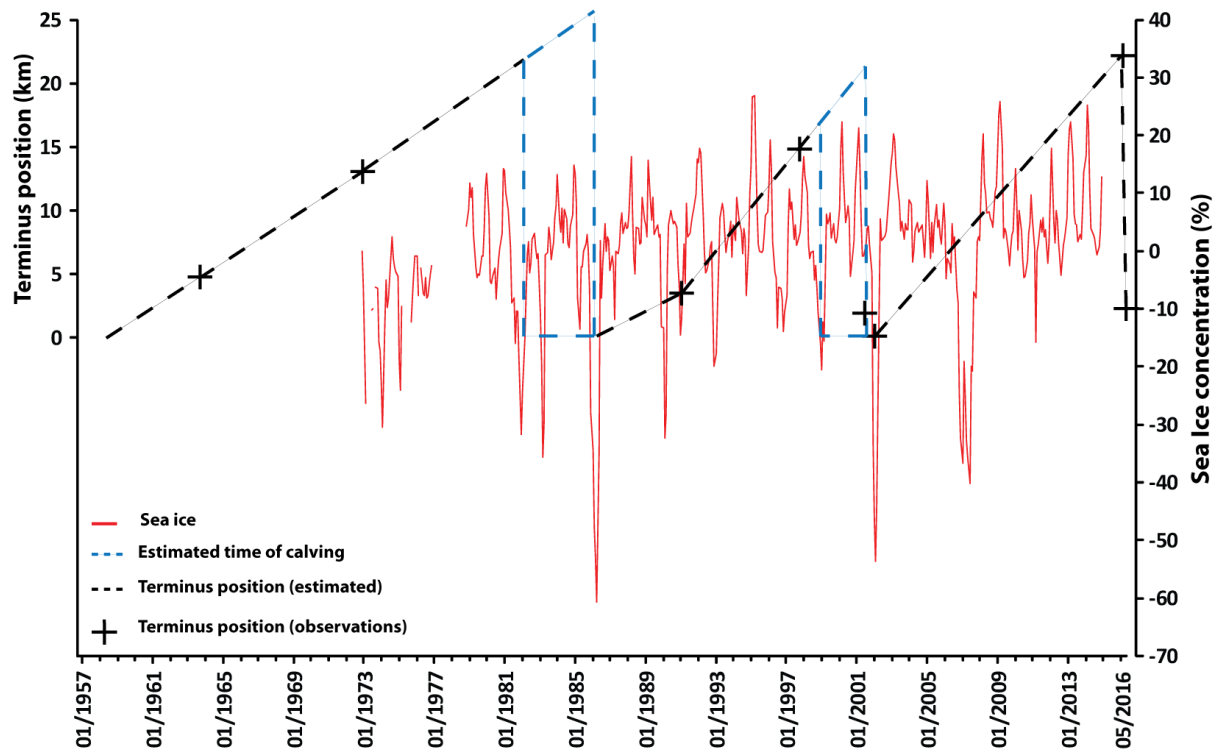
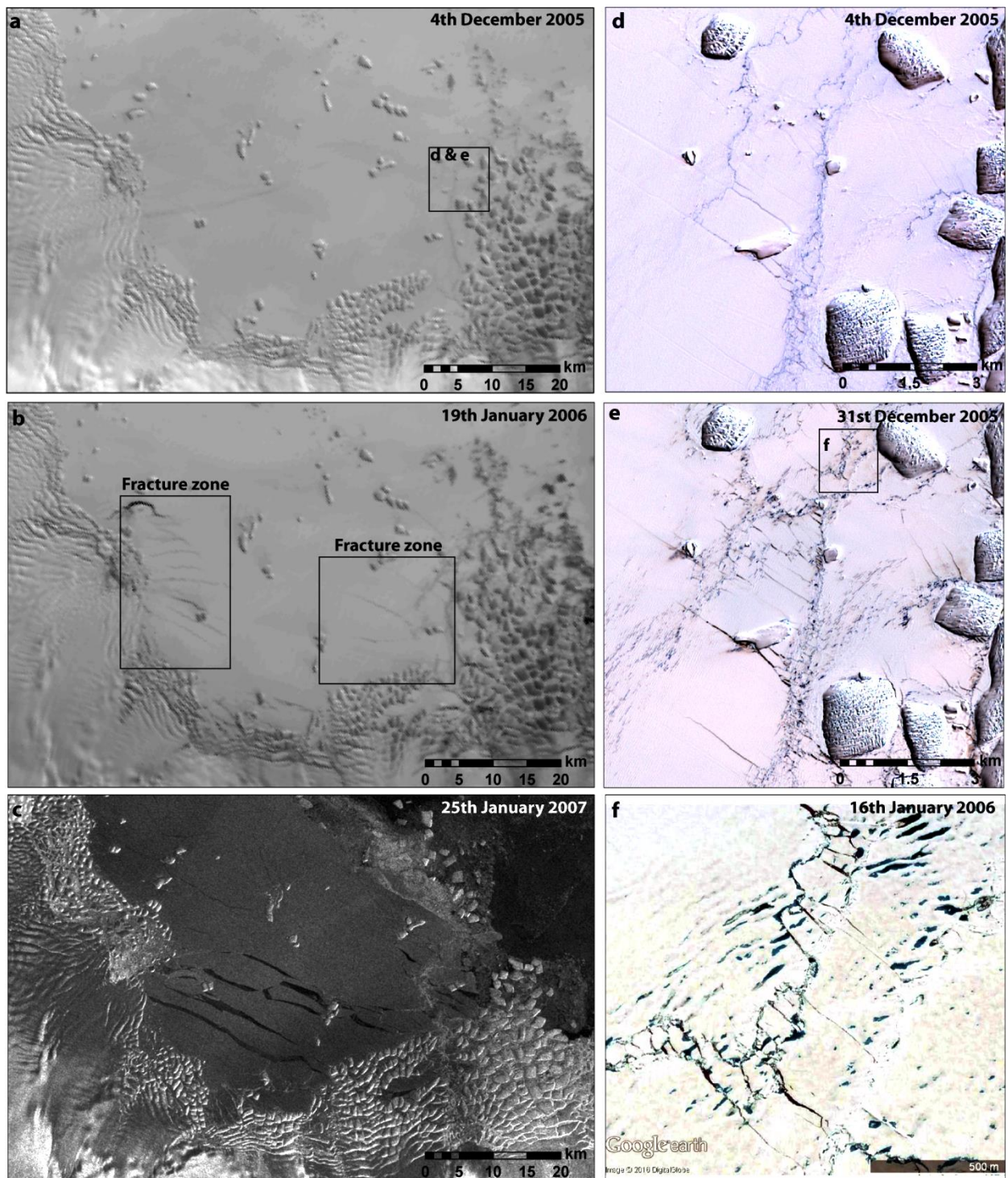


Figure 12: Reconstruction of the calving cycle of Holmes (West) Glacier. All observations are represented by black crosses. The estimated terminus position is then extrapolated linearly between each observation. In periods without observations the date of calving is estimated by negative sea-ice concentration anomalies.



670 **Figure 13: a and b)** Modis imagery showing the development of fractures in the landfast
671 sea-ice between 4th December 2005 and 19th January 2006 ([https://nsidc.org/data/iceshelves](https://nsidc.org/data/iceshelves_images/cgi-bin/modis_iceshelf_archive.pl)
672 [_images/cgi-bin/modis_iceshelf_archive.pl](https://nsidc.org/data/iceshelves_images/cgi-bin/modis_iceshelf_archive.pl)). **c)** The landfast sea-ice ruptures along some of
673 the same fractures which formed in December/January 2005/06, eventually leading to
674 complete break-up in January 2007. **d and e)** ASTER imagery showing surface melt features
675 and the development of smaller fracture between 4th and 31st December 2005. **f)** High

resolution optical satellite imagery from 16th January 2006 showing sea-ice fracturing and surface melt ponding. This image was obtained from Google Earth.

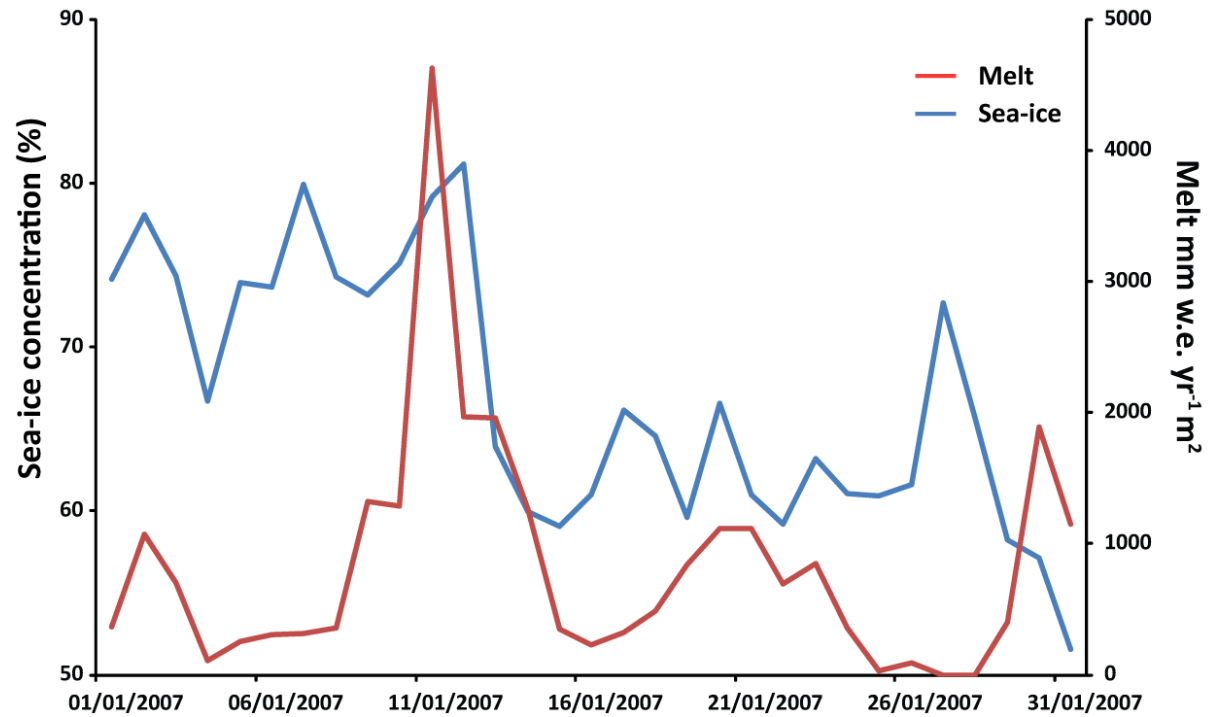


Figure 14: Daily sea-ice concentrations and RACMO derived melt during January 2007 in Porpoise Bay. Sea-ice concentrations start to decrease after the melt peak on January 11th.